Title: Phenotypic characterization of a mouse model of Rett syndrome reveals pubertal dysregulation and hypothalamic-gonadal dysfunction

Authors: Ana Martín-Sánchez[1*#]; Rafael Esteve-Pérez[1], Daniela Jiménez-Díaz[1]; Alexandru Vasile-Tudorache[1]; Jordan E. Read[2]; Sasha R. Howard [2,3]; Carmen Agustín-Pavón[1*]

[1]Dept Cell Biology and Functional Biology, Faculty of Biological Sciences, Universitat de València, València, Spain

[2]Centre for Endocrinology, William Harvey Research Institute, Queen Mary University of London, London, UK

[3]Department of Paediatric Endocrinology, Royal London Children's Hospital, Barts Health NHS Trust, London, UK

[#] Current address: Unitat Predepartamental de Medicina, Universitat Jaume I de Castelló, Castelló de la Plana, Spain

*Corresponding authors

Ana Martín-Sánchez, anamarti@uji.es

Carmen Agustín-Pavón, m.carmen.agustin@uv.es

ORCID

Ana Martín-Sánchez 0000-0002-7046-8886

Rafael Esteve-Pérez 0009-0004-6462-1604

Daniela Jiménez-Díaz 0009-0000-2811-6134

Alexandru Vasile-Tudorache n/a

Jordan E. Read 0000-0001-6731-4440

Sasha R. Howard 0000-0002-6698-903X

Carmen Agustín Pavón 0000-0002-6725-6954

Abstract

Background: Mutations in the *MECP2* gene, encoding the epigenetic reader Methyl-CpG binding protein 2, are the main cause of Rett syndrome, a rare neurodevelopmental disorder. Besides severe symptoms such as profound intellectual disability, loss of speech and motor skills and epilepsy, loss of function of *MECP2* has been associated with pubertal dysregulation, but the biological mechanisms leading to this remain unclear.

Methods: We first carried out a patient survey to assess pubertal timing in a sample of Spanish patients with Rett syndrome. Second, using a mouse model of Rett, in which males are hemizygous and females heterozygous for *Mecp2* loss of function mutation, we assessed the onset and progression of puberty, together with increase in body weight and onset of neurological symptoms in post-weaning mice until puberty. In brain samples of young adult mice, we analysed hypothalamic Gonadotropin releasing hormone (GnRH) neurons by immunofluorescent labelling, and in plasma samples measured circulating GnRH and testosterone concentrations. Finally, we analysed testosterone dependent arginine-vasopressin circuits.

Results: Our data in patients are in agreement with previous reports showing that a subset of female patients with Rett syndrome experience a delayed timing of menarche. Further, in our mouse model we found delayed puberty in *Mecp2* ^{CD1}-null males, associated with a reduced rate of weight gain, but with puberty onset occurring at a lower body weight than in wildtype controls. Despite later puberty onset, *Mecp2*^{CD1}-null male mice were found to have an increased number of GnRH neurons, but displayed lower levels of circulating reproductive hormones. Consequently, *Mecp2*^{CD1}-null males have deficient testosterone-dependent arginine-vasopressin innervation. In female *Mecp2*^{CD1}-heterozygous mice, we found no overall significant differences in pubertal development or GnRH neurons, albeit in a subset of mice with early neurological symptoms, we found lower body weight, and a trend to delayed vaginal opening but precocious first oestrous, attributable to variable phenotypic penetrance.

Conclusions: Our data supports that *MECP2* is essential for typical pubertal development, with complete loss of *Mecp2* in a male murine model resulting in abnormalities of pubertal timing with an observed increase in hypothalamic GnRH neurons.

Keywords

Gonadotropin-releasing hormone, MeCP2, puberty, Rett syndrome, testosterone

Introduction

The X-linked *MECP2* gene encodes the methyl CpG-binding protein 2 (MeCP2), a multifunctional protein first characterised as a transcriptional repressor able to bind to methylated DNA (1) and currently mostly defined as an epigenetic reader with both transcriptionally repressive and activating functions (2) MeCP2 is expressed in a variety of tissues, but it has a fundamental role in the brain, where it is involved in the maintenance of a mature neuronal phenotype (3,4). Thus, mutations in *MECP2* are associated with several neurological disorders (5). In particular, loss of function mutations in *MECP2* are the main cause of Rett syndrome (RTT) (6), a rare neurodevelopmental disorder and one of the most severe conditions linked to this gene. RTT mainly affects girls, who are heterozygous for the mutation; on the contrary, boys suffer a complete loss of *MECP2* and typically die perinatally (5). Girls with RTT, who are born apparently healthy, develop the first symptoms around 6-18 months of age, including an arrest of development followed by loss of acquired skills. The main symptoms are loss of speech, loss of purposeful use of the hands, intellectual disability, epilepsy and progressive loss of ambulation (7). On the other hand, duplication of *MECP2,* causing duplication syndrome (MDS), affects boys, leading also to intellectual disability, motor impairment and epilepsy (7).

In addition to these severe symptoms, loss of function of *MECP2* can lead to endocrine dysregulation, which can contribute to emotional symptoms (8), and disordered puberty (9). Related to this, a handful of studies have reported cases of patients with RTT or MDS that display precocious puberty(10–12). Recently, rare variants of *MECP2* were identified in patients with central precocious puberty with isolated neurodevelopmental features including autism or microcephaly, but without RTT (13). Further, pubertal trajectories have been seen to be altered in a subset of patients with RTT, with around 20% of females experiencing precocious onset of puberty but delayed menarche (9). This extended course of puberty, with early breast development but late pubertal completion, is also observed in disrupted oestrogen signalling such as from exposure to estrogenic endocrine-disrupting chemicals (14).

The onset of puberty is triggered by the activation of hypothalamic neurons containing Gonadotropin Realising Hormone (GnRH) (15). These neurons are neuroendocrine cells that develop within the nasal placode and reside in the olfactory bulbs, septum and the preoptic and anterior regions of the hypothalamus in the adult mammalian brain(16). GnRH hypothalamic neurons, via pulsatile GnRH signalling, regulate the gonadotrope cells of the hypophysis, which release luteinizing hormone (LH) and follicle stimulating hormone (FSH). In turn, LH and FSH control the production and release of gonadal

hormones (oestradiol, testosterone), which provide negative (and positive) feedback signalling to the hypothalamus-pituitary to coordinate pubertal development and adult reproduction.

Several potential pathways exist via which *MECP2* could influence GnRH activation. Firstly, by means of its transcriptional control of FXYD domain-containing transport regulator 1 (*FXYD1*), a protein responsible for control of GnRH neuronal excitability. Patients with RTT and *Mecp2*-null mice demonstrate a pathogenic overexpression of *FXYD1* in the frontal cortex of the brain, attributed to lack of repression by *MECP2* (17), and mRNA levels of *Fxyd1* in rat brain closely correlate with increased GnRH neuron excitability at puberty and first oestrus (18). Next, as an epigenetic regulator, MeCP2 regulates gene expression through interaction with both 5-methylcytosine (5mC) and 5-hydroxymethylcytosine (5hmC) residues in DNA, impacting chromatin accessibility, recruiting histone modifying enzymes and forming part of various polycomb complexes (19–21). Beyond the traditional idea of MeCP2 as a repressor of gene expression through its association with 5mC, it has also been found to associate with active chromatin regions, enriched at 5hmC loci in neurons. The Rett syndrome *MECP2* variant p.R133C preferentially disrupts the association with 5hmC (21). Likewise, MeCP2 has demonstrated a strong co-localisation within the mouse cortex with repressing histone mark H3K27Me3 (20) as well as an association with the activating histone mark H3K4Me3 (19), indicating a role as both an activator and repressor of gene expression. Additionally, evidence for estrogen receptor-β and estrogen receptor-related receptor-α (Erα and Erβ) expression in murine GnRH neurons suggests a direct role for estrogen signalling in the regulation of GnRH secretion (22). MeCP2 is seen to associate with the Erα promoter in mouse cortex, correlating with increased promoter methylation and reduced Erα expression beyond postnatal day 10 (P10). Female mutant *Mecp2* mice demonstrate an increase in this Erα expression beyond P10, inverse to the reduced levels seen in wildtype mice, suggesting a mis-regulation of Erα expression upon loss of functional *Mecp2* (23).

Mecp2-mutant mice are valuable model systems for the study of RTT (24). In contrast to humans, loss of function mutation is not lethal to males, so *Mecp2*-null male mice survive into young adulthood, albeit developing severe motor impairment and reduced lifespan (24). The onset of symptoms in *Mecp2*-heterozygous females is variable, with some of them displaying mild behavioural symptoms at young age and others remaining pre-symptomatic until 4-6 months of age (8,25). Aside from the typical motor symptoms, in the first report describing the model, Guy and collaborators (24) noted that *Mecp2*-null males had universally undescended testicles and were infertile. In agreement with this

anecdotal report, young adult *Mecp2*-null males displayed low levels of testosterone-dependent features, such as aggression, arginine-vasopressin (AVP) sexually dimorphic central circuits and production of male pheromones (26). These data strongly suggest that *Mecp2*-mutant mice could help to understand the mechanisms of altered pubertal development observed in patients, but, to our knowledge, this has not been previously investigated.

Thus, in this study, we first sought to gain more human data on the possible altered pubertal trajectory in patients with RTT, by means of a survey of pubertal timing among Spanish parents and carers. Second, we sought to characterize the pubertal trajectories, analyse GnRH neuronal circuitry and the levels of circulating sex hormones in a relatively novel model of *Mecp2* mutant mice on CD1 background, a model that maximizes colony productivity (27).

Material and methods

Patient survey

We conducted a survey between February and May 2023 among parents and carers of Rett Syndrome patients from the Asociación Española de Síndrome de Rett (AESR) and Associació Catalana de Síndrome de Rett (ACSR), asking them the age of the first menstrual period of female patients. We collected data from a cohort of 42 Spanish female patients aged between 8 to 49 years old (average age 21.5±11.1, S.D.). The inclusion parameters were: Spanish-born girls, *MECP2* mutation and older than 8 years of age (none of the patients surveyed had reached menarche before the age of 8 years) (28). All data were treated according to the Spanish Law of Protection of Personal Data and Guarantee of Digital Rights of December 5th, 2018 (BOE-A-2018-16673). Parents and carers provided and signed an informed consent form, and the survey was approved by the Ethics Committee on Human Experimentation from the University of Valencia.

Animals and rearing conditions

For the present study, we used mice model of RTT from a genetically modified strain derived in our facilities from a commercial line. Briefly, we crossed *Mecp2*-heterozygous females bred in-house (B6.129P2(C)-Mecp2$^{tm1.1Bird/J}$, The Jackson Laboratory) with pure CD1 males (Crl:CD1(ICR), Charles River Laboratories) for more than 10 generations, following (27). Animals were housed with *ad libitum* water and food in a room maintained at 22 ± 1ºC, humidity 55 ± 10% and a12:12 h light/dark cycle, with lights on at 08:00h. All experimental procedures were approved by the Committee of Ethics and Animal Experimentation of the Universitat de València and treated according to the European Union Council Directive of June 3rd, 2010 (6106/1/10 REV1) and under an animal-usage

license issued by the Direcció General de Producció Agrària i Ramaderia de la Generalitat Valenciana (2022/VSC PEA/0288).

Genotyping and expression of MeCP2 in the brain

For genotyping, we obtained ear biopsies at weaning and after DNA extraction we applied the protocol supplied for this strain by the Jackson Laboratory. To further check the maintenance of loss of expression of *Mecp2* in the new strain, we carried out an immunofluorescent detection of MeCP2 in a WT and *Mecp2*^{CD1}-null males (Supplementary material, Figure S1).

Weight gain, onset of neurological symptoms

Animals were weighed daily due to its relation to symptom development and influence on the onset of puberty, and checked for hindlimb clasping by lifting them gently by the tail, as a proxy of neurological symptoms (24,29).

Puberty onset, oestrous cycle monitoring and gonadal histology

Puberty was determined by the day of vaginal opening in females and balanopreputial separation in males, respectively, from postnatal day 25 (P25) (females, WT, n= 14, *Mecp2*^{CD1}-het, n= 9; males: WT, n=16; *Mecp2*^{CD1}-null, n=21) (30,31). Balanopreputial separation in males was assessed by gently attempting manual retraction of the prepuce. For females, those mice that exhibited hindlimb clasping behaviour were classified as *Mecp2*^{CD1}-het symptomatic (*Mecp2*^{CD1}-het Symp). By contrast, *Mecp2*^{CD1}-het females that did not show clasping behaviour were classified as *Mecp2*^{CD1}-het non-symptomatic (*Mecp2*^{CD1}-het NonS). Additionally, we determined the occurrence of the first oestrous and oestrous cyclity by collecting vaginal smears for 10 days after vaginal opening, following (32). Briefly, vaginal cells were collected by gently flushing the external vaginal area with a small amount (50-100 µl) of saline solution (NaCl 0.9%, Braun), using a pipette inserted into a sterile latex bulb. The liquid was slowly released into the vaginal opening and then drawn back into the pipette using the bulb. The process was repeated 4-5 times using the same solution until the resulting fluid became turbid. Then, the solution with cell suspension was dropped over a glass slide, dried using a hot plate, and counterstained using a toluidine blue (Sigma-Aldrich) 0.25% solution.

Shortly after completion of puberty, a subset of mice was sacrificed, and gonads removed, postfixed in PFA 4% and stored with 70% ethanol solution, included in paraffin, sectioned in 10µm-thick sections and counterstained with haematoxylin-eosin.

Analysis of GnRH neurons

Perfusion, fixation and tissue sectioning

At two months old, an age considered in mice as young adulthood with full reproductive capacity (33), animals (females, WT, n= 3, *Mecp2*^{CD1}-het, n= 3; males: WT, n=5; *Mecp2*^{CD1}-null, n=7) were deeply anaesthetized using a dolethal overdose (i.p. injection

of 0.02 mg/g of body weight of pentobarbital-based solution). Then, animals were euthanized by transcardiac perfusion of phosphate saline solution 0.1 M (PBS 0.1M, pH 7.4) using a peristaltic pump (5.5 ml/min for 2 min) followed by 4% paraformaldehyde in 0.1 M PBS, pH 7.4 (same flux for 5 min). Brains were carefully removed and immediately post-fixed in the same fixative solution overnight at 4ºC. Then, brains were cryoprotected (30% sucrose solution in 0.1 M PBS, pH 7.6, 4ºC) and cut into five sets of 40µm-thick coronal sections using a freezing microtome (Leica SM 2010R) and stored with 30% sucrose and 0.02% sodium azide in 0.1 M PB at -80ºC.

Immunofluorescence for GnRH

One of the five parallel coronal series obtained from young adult mice were purposed for GnRH immunofluorescence. Free-floating sections were washed with 0.05 M TRIS buffered saline pH 7.6 (TBS) (3 × 10 min). In brief, sections were: (i) incubated in 1% $NaBH_4$ in TBS to prevent tissue auto-fluorescence for 30 min at RT; (ii) pre-incubated in 3% normal donkey serum (NDS; Sigma-Aldrich, G9023) in TBS with 0.2% Triton X-100, at RT for 1 h, to block nonspecific labelling; (iii) incubated in monoclonal rabbit anti-GnRH primary antibody (1:5000, Invitrogen, AB1567) diluted in TBS; (iv) incubated with fluorescent-labelled RedTM-X-conjugated at a 1:500 dilution (Jackson ImmunoResearch, 711- 295-152) secondary antibody (90 min at RT) diluted in TBS. To reveal the cytoarchitecture in brain sections, they were counterstained prior to mounting by 5 min washes in 4',6- diamino-2-fe-niindol (DAPI, a nuclear staining) at a 1:10000 dilution. After each step, sections were washed 3 times for 5 min in TBS except between step (ii) and (iii). Finally, sections were washed in TB, mounted onto gelatinised slides and cover-slipped with fluorescence mounting medium FluorSave Reagent (Sigma-Aldrich, 345789).

Determination of circulating hormonal levels

Blood samples from young adult male mice (WT, n=5; *Mecp2*^{CD1}-null, n=7) were obtained from the aortic arch immediately before perfusion (between 10:00 a.m. and 13:00 a.m.) and under anaesthesia conditions. These samples were collected into heparinized tubes, which were rapidly centrifuged at 20.000 g for 15 min at RT (Eppendorf 5424 Centrifuge), until plasma was separated from blood cells. Supernatant (100 µl) was collected and immediately stored at -80C until used. Samples selected for ELISA were processed according to the protocol supplied by the ELISA kit manufacturer for testosterone (Bio-Techne R&D Systems, S.L.U. KGE010) and GnRH (ElabScience, E-EL-0071) determination. Optical density was read at 450 nm in a Thermo Scientific Multiskan FC automatic spectrophotometer. Concentrations were calculated using their standard curves.

Arginine vasopressin immunohistochemistry

We performed an immunostaining for AVP in a subset of one of five parallel sets (WT, n = 3; *Mecp2*^{CD1}-null, n = 3) as previously published (26). Briefly, sections were washed three times with 0.05 M TBS for 5 min. Then, they were incubated sequentially in: (i) 1% H_2O_2 in 0.05 M TBS pH 7.6 for 30 min at RT for endogenous peroxidase inactivation; (ii) blocking solution, 0.05 M TBS pH 7.6 with 0.3% Triton X-100 and 2% normal goat serum; (iii) primary antibody (1:10,000, rabbit anti-vasopressin IgG, Chemicon, AB1565) overnight at 4 °C; (iv) diluted biotinylated secondary antibody (1:200, goat anti-rabbit IgG, Vector Labs, BA-1000) in TBS for 90 min at RT; (v) avidin–biotin–peroxidase complex (ABC Elite kit; Vector Labs, PK-6200) in TBS for 90 min at RT. Between each step, sections were washed in TBS (3 × 10 min) except after step (ii). After ABC incubation, sections were rinsed in TBS (3 × 10 min) and TRIS buffer (TB) 0.05 M, pH 8 (3 × 10 min). The histochemical detection of the resulting peroxidase activity was performed by incubation in 0.003% H_2O_2 and 0.025% 3,3-diaminobenzidine (Sigma) in TB for about 15 min. The sections were finally rinsed thoroughly in TB, mounted onto gelatinized slides, dehydrated in ethanol, cleared with xylene and coverslipped with Entellan.

Microscopy and image acquisition

Brain and gonadal samples were analysed using a microscope equipped with light and fluorescent lamps (Leica Microsystems series 140269 LEITZ DMRB microscope, digital camera LEICA DFC495). Fiji-ImageJ software was employed to manually quantify the number of GnRH-positive and AVP-ergic cells using the *cell counter* plugging and to identify the percentage of area occupied by AVP-ergic innervation. No manipulations of individual image elements were carried out.

Statistical analysis

Data were analysed using IBM SPSS Statistics 23.0 and GraphPad Prism. We first checked the data for normality (Kolmogorov-Smirnov's test) and homoscedasticity (Levene's test). We performed t-Student tests, one-way ANOVAs and ANOVA for repeated measurements to analyse the weight variation across different ages. Log-rank test was used to evaluate differences in the observation of first oestrous in female mice. When applicable, pairwise comparisons were analysed with Bonferroni's correction. When data were not normally distributed, Fischer's test was used for the balanopreputial separation data. Statistical differences were considered significant when $p < 0.05$.

Results

The age of menarche is delayed in Spanish patients with RTT

Of the cohort of female patients with RTT, 30.95% (13 out of 42, 10.23±1.91 years old) had not yet achieved menarche. The remaining 29 patients had experienced menarche

at varying ages (Table 1). Of those 29 patients, 13 of them (30.95% of the whole cohort) experienced a delayed menarche, defined as girls reaching menarche after the age equivalent to the 80th percentile for age at menarche of the healthy population (13.2 years), according to data from the Spanish Association of Paediatrics (28). A Student t-test comparing the average age of menarche for patients with RTT with the average age in that study for healthy Spanish adolescents revealed significant differences between the groups (t_{28} = 2.15; p = 0.04). No data were available for timing of pubertal onset (breast development).

Table 1. Comparison of age at menarche between Spanish patients with RTT and previously published data of healthy Spanish females. The percentage of girls with RTT experiencing delayed menarche was calculated as the % of girls from the RTT sample reaching menarche above the 80th percentile for age at menarche for healthy Spanish females (28).

	n	Average age at menarche	Range of age at menarche	% of patients delayed menarche
Healthy Spanish females*	198	12.42±1.01	9.9 – 15.6	21.1 %
RTT patients	42	13.34±2.36	10 - 20	31 %

The weight of pubertal *Mecp2^{CD1}*-mutant mice is affected by sex and onset of neurological symptoms

The weight of female *Mecp2^{CD1}*-het mice increased with postnatal days ($F_{3,23}$= 395.08, p < 0.001, Figure 1a), with no differences compared to WT controls. By contrast, in *Mecp2^{CD1}*-null males, we found a significant effect of the factor *Day* ($F_{3,33}$= 467.61, p < 0.001) and of the factor *Genotype* in ($F_{1,35}$= 1118.46, p < 0.001), indicating that *Mecp2^{CD1}*-null male mice showed an overall lower weight in comparison to control littermates (Figure 1b). With respect to neurological symptoms, we found that 81% of *Mecp2^{CD1}*-null males displayed hindlimb clasping at least once during the observation period (P25 to P35), whereas for female *Mecp2^{CD1}*-het mice this percentage was 55%. To determine whether the onset of neurological symptoms was associated to other phenotypic measures, we split the *Mecp2^{CD1}*-mutant mice into symptomatic (Symp) and non-symptomatic (NonS) groups. In both sexes, weight at P25 was significantly different among groups (one-way ANOVA, $F_{2,24}$ = 8.344, p < 0.01; Figure 1a' for females; one-way ANOVA, $F_{2,34}$ = 15.36, p = 0.002; Figure 1b'' for males). In both sexes, *Mecp2^{CD1}*-mutant Symp showed lower weight in comparison to *Mecp2^{CD1}*-mutant NonS (p = 0.001 for females; p = 0.021 for males) and WT (p = 0.019 for females; p < 0.001 for males) littermates.

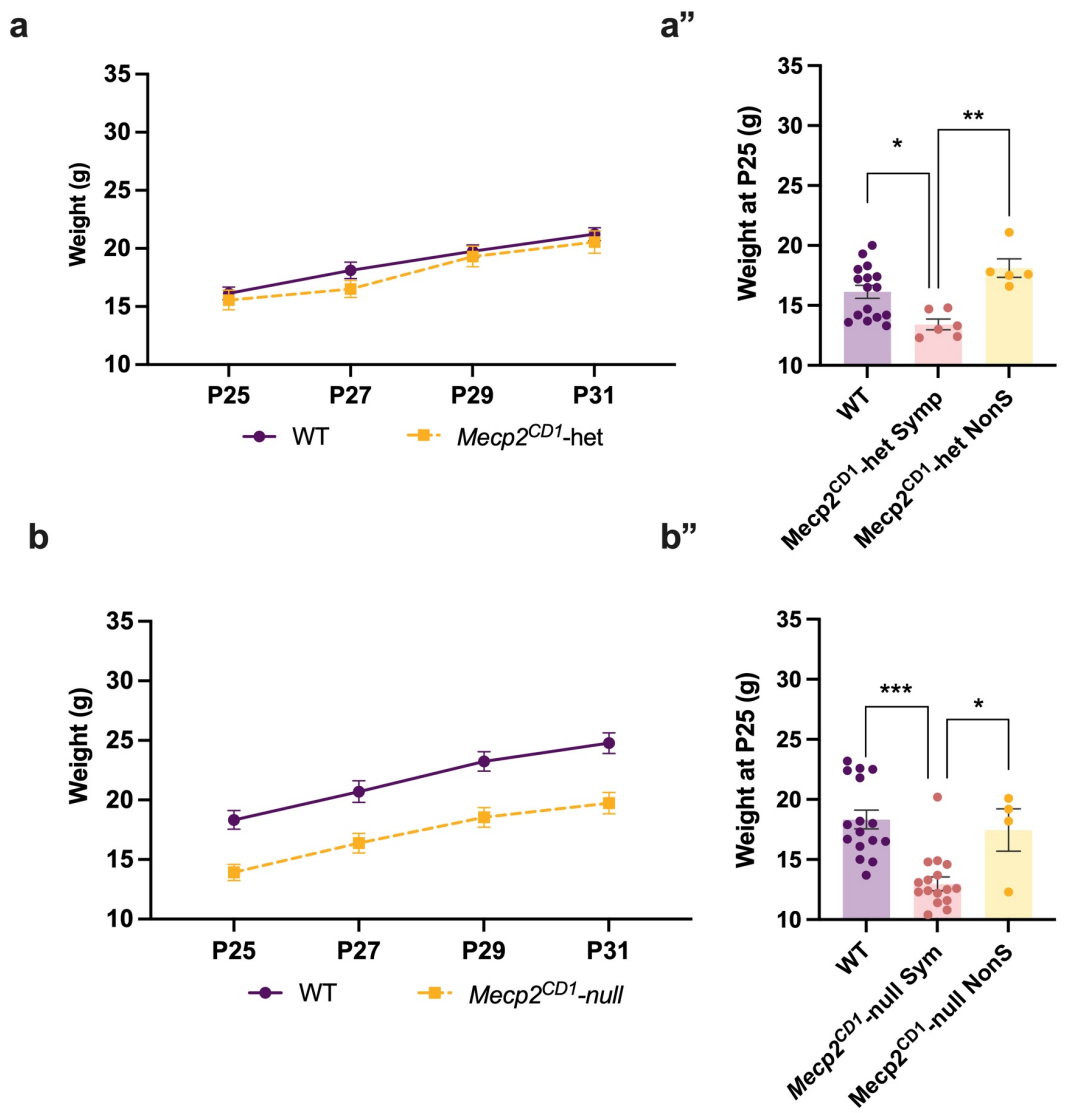

Figure 1. Weight gain and symptom onset in *Mecp2^{CD1}*-mutant mice. Graphical representation of body weight gain in *Mecp2^{CD1}*-het females (n=11) (a) and *Mecp2^{CD1}*-null males (n=16) (b) in comparison with their WT control mice (n=16 for females; n=21 for males). *Mecp2^{CD1}*-mutant symptomatic mice showed a reduction of weight on PD25 when compared to *Mecp2^{CD1}*- mutant non-symptomatic and WT mice (a', b'). Data are shown as Mean ± S.E.M. * $p < 0.05$; ** $p < 0.01$; *** $p < 0.001$.

Timing of the onset of puberty is not significantly affected in *Mecp2^{CD1}*-het females

We monitored the initiation of puberty by means of the external marker of vaginal opening in females (Figure 2a) daily from P25. No significant differences in timing of vaginal opening were seen between *Mecp2^{CD1}*-het females and their WT counterparts (t-Student test, $p > 0.05$, Figure 2a). The weight of all *Mecp2^{CD1}*-het females was similar to WT females at the day of vaginal opening ($p > 0.05$, Figure 2b). However, when *Mecp2^{CD1}*-het females were classified with respect to symptom onset, data revealed a trend toward

delayed vaginal opening in *Mecp2*^{CD1}-het Symp (one-way ANOVA, $F_{2,24} = 2.71$, $p = 0.087$, Figure 2c). Finally, we failed to detect any significant effect of genotype on first estrous, cycle length, or estrous cyclicity in *Mecp2*^{CD1}-het females ($p > 0.05$ in all cases, Figure 2d, e and f, and Supplementary Figure S2), albeit we found oestrus in *Mecp2*^{CD1}-het Symp was slightly advanced (Figure 2d). Finally, we did not find gross abnormalities in the gonads of adolescent female mice, finding follicles in all stages of development (Figure 2g and g').

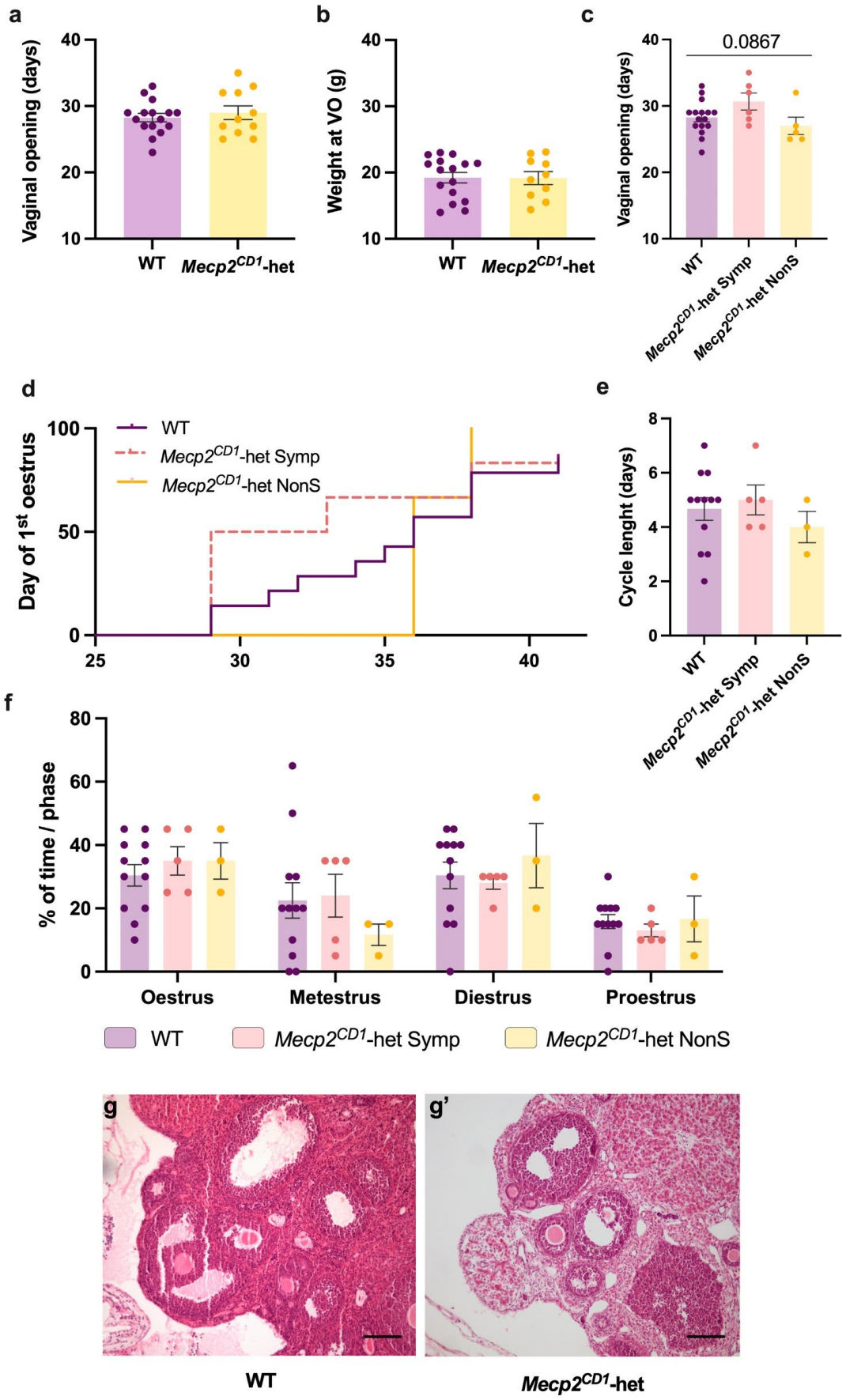
a
Vaginal opening (days)
40
30
20
10
WT
Mecp2CD1-het
b
Weight at VO (g)
40
30
20
10
WT
Mecp2CD1-het
c
Vaginal opening (days)
0.0867
40
30
20
10
WT
Mecp2CD1-het Symp
Mecp2CD1-het NonS
d
Day of 1st oestrus
100
50
0
25
30
35
40
WT
Mecp2CD1-het Symp
Mecp2CD1-het NonS
e
Cycle lenght (days)
8
6
4
2
0
WT
Mecp2CD1-het Symp
Mecp2CD1-het NonS
f
% of time / phase
80
60
40
20
0
Oestrus
Metestrus
Diestrus
Proestrus
WT
Mecp2CD1-het Symp
Mecp2CD1-het NonS
g
g'
WT
Mecp2CD1-het

Figure 2. Pubertal development in *Mecp2^{CD1}*-het females. a) Days to vaginal opening (VO) in WT and all *Mecp2^{CD1}*-het females and (b) and the weight at VO. *Mecp2^{CD1}*-het symptomatic (*Mecp2^{CD1}*-het Symp) showed a trend toward delayed VO (c) but slightly advanced first oestrous (d) in comparison with *Mecp2^{CD1}*-het non-symptomatic (*Mecp2^{CD1}*-het NonS) and WT littermates. Cycle length (e) and (f) the percentage of time in each oestral cycle phase across 10 days of monitoring reveal no differences between groups. Histological images of representative WT (g) and *Mecp2^{CD1}*-het (g') ovaries are shown. Data are shown as Mean ± S.E.M. * $p < 0.05$. Scale bar: 50µm

The onset of puberty is delayed in *Mecp2^{CD1}*-null males

We monitored the onset of puberty by means of the external marker of balano-preputial separation in males from P25 (Figure 3a). *Mecp2^{CD1}*-null males showed a significant delay in balanopreputial separation when compared to WT animals ($U= 95.50$, $p < 0.05$, Figure 3a). Further, balanopreputial separation occurs in *Mecp2^{CD1}*-null males at a lower body weight than WT controls ($p < 0.001$, $t_{33} = 3.83$; Figure 3b). Of note, and unlike the *Mecp2*-null males on B6.129 background, the testes of young adult *Mecp2^{CD1}*-null males were descended and visible, but they were significantly smaller than those of WT (WT, 7.9±0.37 mm, *Mecp2^{CD1}*-null, 7.3±0.21 mm; 7.8 ± 2.7% reduction in *Mecp2^{CD1}*-null with respect to the average length of WT, one sample t-test, $t_6 = 2.87$, $p = 0.03$) and of lower weight (WT, 0.11±0.01 g, *Mecp2^{CD1}*-null, 0.09±0.01 g; 12.9 ± 6.9% reduction in *Mecp2^{CD1}*-null with respect to the average WT, one sample t-test, $t_6 = 1.86$, $p = 0.11$). However, we did not find gross abnormalities in the gonads of pubescent male mice, observing Leydig cells and spermatocytes in both genotypes (Figure 3c and c').

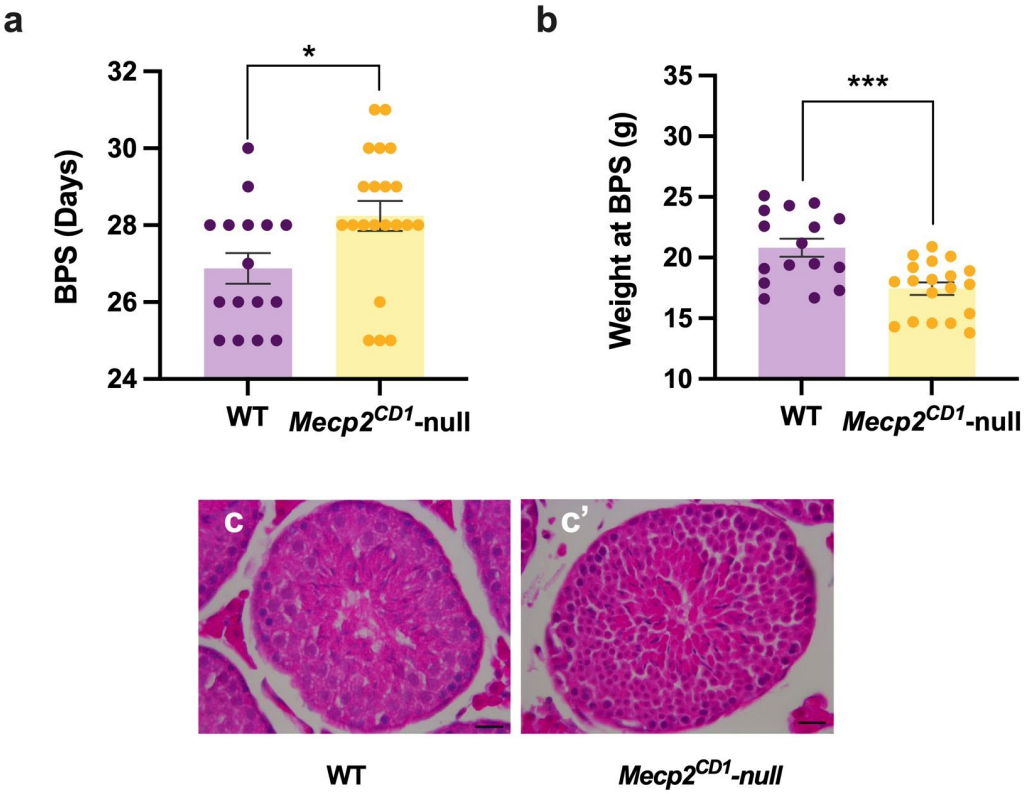

Figure 3. Pubertal phenotype is delayed in *Mecp2*^{CD1}-null males. a) Days to balanopreputial separation (BPS) in WT and *Mecp2*^{CD1}-null males and b) weight at BPS. Histological representative images of WT (c) and *Mecp2*^{CD1}-null (c') testes. Data are shown as Mean ± S.E.M. * $p < 0.05$; *** $p < 0.001$. Scale bar: 20µm

The density of GnRH neurons is increased in young adult *Mecp2*^{CD1}-null males

Subfertility and aberrant sexual development had been previously linked to the early loss of GnRH neurons in a mouse model of Trisomy 21 (34). Hence, we analysed the distribution and density of GnRH neurons in young adult mice. Qualitatively, we found a low number of GnRH-immunoreactive (ir) neurons in the olfactory bulbs (not shown), the septal area and the rostral hypothalamus (Bregma 0.5 to 0.02 mm (35)), with no notable differences between genotypes or sexes (Figure 4a, a', c, c'). Further, we corroborated that GnRH neurons co-expressed MeCP2 in WT mice (Supplementary Figure S3a), but, as expected, some GnRH neurons did not express this protein in *Mecp2*^{CD1}-het females (Supplementary Figure S3b). Quantitatively, and in agreement with the lack of effect on puberty onset of *Mecp2* mutation in heterozygosity in females, the density of GnRH neurons was not significantly different between *Mecp2*^{CD1}-het females and their WT controls ($p > 0.05$, Figure 4b). In contrast, we found an increase in GnRH neurons in *Mecp2*^{CD1}-null as compared to WT male mice ($t_{10} = 2.83$; $p = 0.018$, Figure 4d).

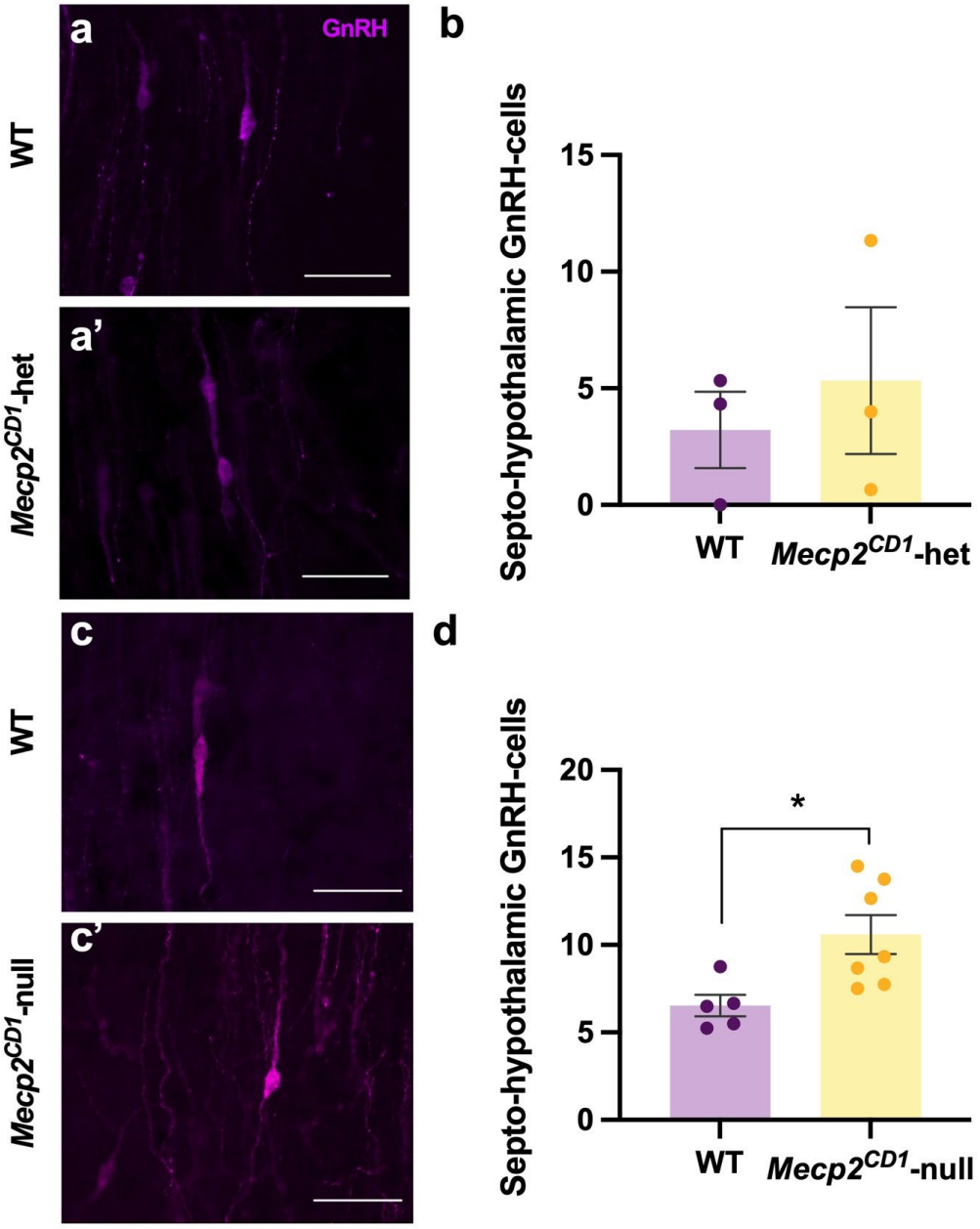

Figure 4. Septo-hypothalamic GnRH-positive cells are increased in *Mecp2*^{CD1}-null male mice. We did not find qualitative differences in the distribution of GnRH-positive neurons, that were found in the septo-hypothalamic area (Bregma 0.5 to 0.02mm) in all groups of mice (a, a', c, c'). GnRH density was not statistically different between WT and *Mecp2*^{CD1}-het females (b), whereas the number of GnRH neurons was significantly increased in mutant males as compared to WT controls (d). Data are shown as Mean ± S.E.M. * $p < 0.05$. Scale bar: 50µm

Circulating levels of reproductive hormones are reduced in young adult *Mecp2*^{CD1}-null males

Given the excess of GnRH neurons in males, we sought to analyse whether this could lead to increased levels of circulating hormones. However, we found that relative circulating levels of GnRH showed a trend toward reduction in *Mecp2*^{CD1}-null as compared to WT males ($t_{12} = 2.08$; $p = 0.06$; Figure 5a). Further, and in agreement with previous data, relative testosterone levels were significantly lower in *Mecp2*^{CD1}-null males compared to controls ($t_{21} = 2.33$; $p < 0.05$, Figure 5b). In a previous study using *Mecp2*-null males on B6.129 background, we found significantly decreased testosterone-dependent AVP-ergic innervation in those mice (26). Here, we replicated this measure in *Mecp2*^{CD1}-null males, where AVP-ergic innervation was almost absent in the lateral habenula of mutant males ($t_3 = 3.02$; $p < 0.05$, Figure 5c, d and d'). As in our previous study, this reduction appears to be specific to testosterone-dependent innervation, since the number of AVP cells in the paraventricular nucleus of the hypothalamus is similar in *Mecp2*^{CD1}-null males and controls, thus not affected by genotype ($p > 0.05$; Figure 5e, f, f').

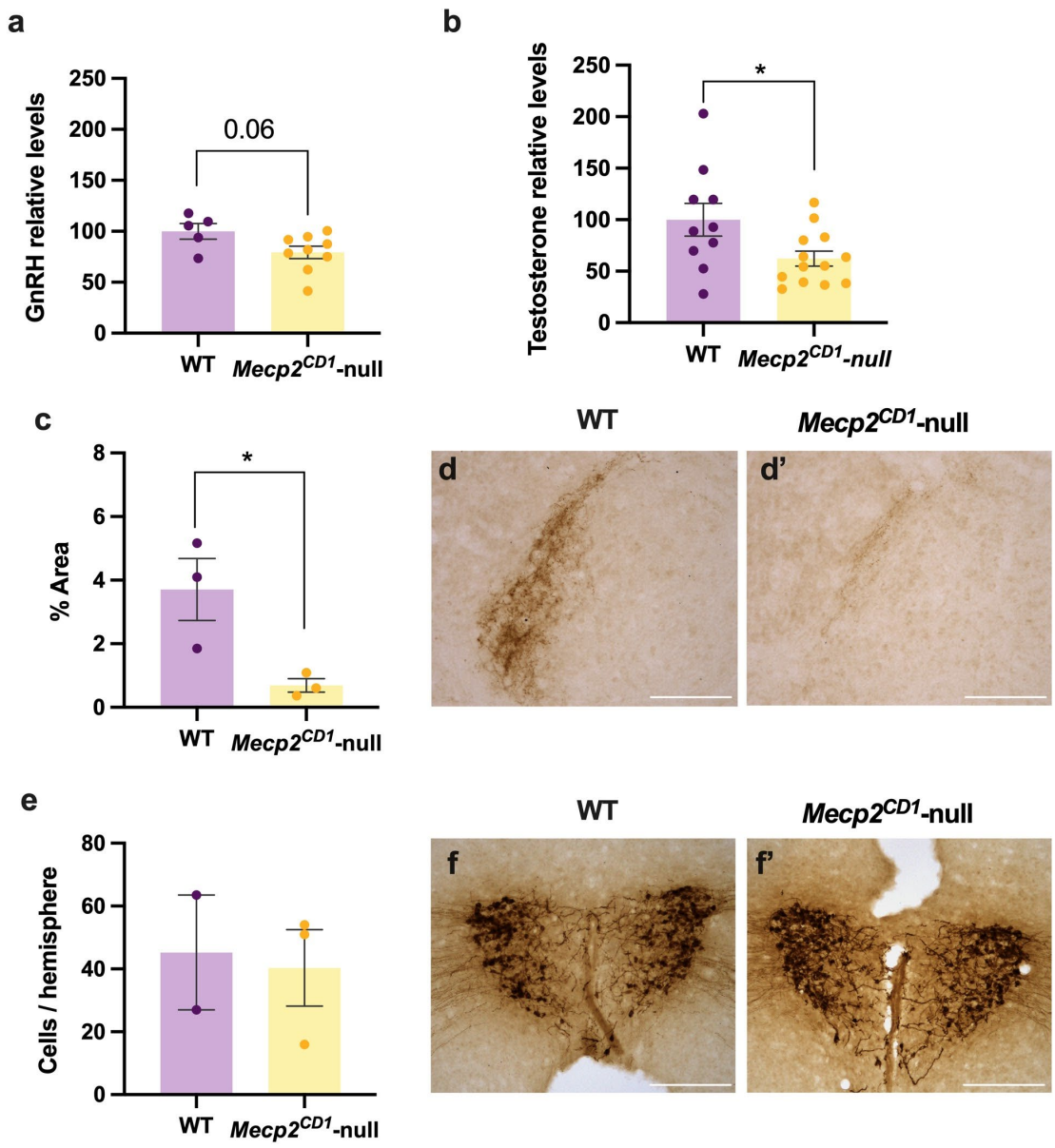

Figure 5. Circulating reproductive hormones and vasopressinergic-testosterone dependent innervation are reduced in adult *Mecp2*^{CD1}-null males. Graphs show relative circulating GnRH (a) and testosterone levels (b). Testosterone-dependent AVP-ergic innervation in habenula in *Mecp2*^{CD1}-null males is significantly reduced in comparison to WT animals (c, d and d'). By contrast, the density of AVPergic cells in the paraventricular nucleus of the hypothalamus is not affected by genotype (e, f, f'). Data are shown as Mean ± S.E.M. * $p < 0.05$. Scale bar: 50µm

Discussion

In this work, we sought to study pubertal dysregulation in RTT syndrome via a patient survey and the characterization of a relatively novel mouse model deficient for *Mecp2*. First, we obtained results in keeping with a previous study (9), finding that female patients

with RTT may experience delayed menarche with a higher prevalence as compared to the healthy population. In the mouse model, the *Mecp2*^{CD1}-null, derived to CD1 strain from the original B6.129 *Mecp2*-null, we found the expected effects of *Mecp2* loss on body weight and hindlimb clasping. In females, we had a lower proportion of symptomatic animals at young ages than in males and found mild effects on pubertal development which depended on symptom severity. By contrast, in males, we found a significant delay in achieving pubertal milestones in *Mecp2*^{CD1}-null males as compared to their WT counterparts, a delay that may be influenced by the significantly lower weight during infancy and pubescence in these males. Finally, we found an excess of GnRH neurons in the septo-hypothalamic region in young adult *Mecp2*^{CD1}-null males, contrasting with lower circulating levels of sex steroid hormones of the hypothalamic-hypophyseal-gonadal axis.

Although RTT syndrome is defined as a neurodevelopmental disorder, it is in fact a multiorgan disease affecting multiple systems in the body, causing gastrointestinal and orthopaedic problems, altered immune response and endocrine comorbidities (36–38). The most common symptoms related to endocrine dysfunction are low bone mineral content, malnutrition (which could be also related to motor impairment causing difficulties in eating) and alterations in the initiation of puberty (9,36,38,39). With regards to puberty timing, data are scarce and conflicting. Various longitudinal population-based studies suggest that a subset of patients with RTT (3-6%) experience premature menarche (9,40), particularly those with milder mutations in the *MECP2* gene (9). In contrast, 19% of girls were found to experience a delayed menarche (9), a percentage close to the result in our study (31%). Overall, these data from human patients with RTT suggest that the disease is associated with deviations from normal pubertal timing, with some patients experiencing early onset but delayed completion (9).

Body weight and nutrition have a strong influence on pubertal timing and reproductive health (41), and both patients with RTT and the mouse model studied here are likely to be affected by these factors. Indeed, *Mecp2*^{CD1}-null males showed a significantly lower weight than healthy controls at all stages, and a significantly delayed balanopreputial separation, which occurred at lower body weight, in comparison to WT males. Interestingly, testes of *Mecp2*^{CD1}-null males with CD1 background are not internal, unlike previous *Mecp2*-null male mouse models, but were smaller and lighter than testes of WT males.

Of note, a high percentage of *Mecp2*^{CD1}-null displayed neurological symptoms at a young age (24,42). The early onset of the disease in this model was expected in males, in which the complete loss of *Mecp2* strongly affects most phenotypes (26,43) and reduces the

lifespan of these mice (24); thus, low weight and ill health might have a profound influence on the pubertal development in mutant males.

By contrast, in our cohort of *Mecp2*^{CD1}-het females, body weight was, overall, not significantly different from WT controls; unless we took into consideration whether these mice were displaying the neurological symptom of clasping by the time of phenotypical assessment in this study. Thus, *Mecp2*^{CD1}-het Symp mice were significantly lighter than their WT controls and their *Mecp2*^{CD1}-het NonS at the first day of observation, and this lower weight might have contributed to a slightly delayed vaginal opening in *Mecp2*^{CD1}-het Symp compared to *Mecp2*^{CD1}-het NonS. By contrast, the first oestrous, a measure which more accurately reflects the onset of human puberty than vaginal opening, was slightly advanced in *Mecp2*^{CD1}-het Symp. An atypical pubertal development showing a delay in vaginal opening but an advanced first oestrus, would be in agreement with patient data relating rare variants of *MECP2* with central precocious puberty (13) and Rett with altered pubertal trajectories (9). However, the relatively low number of females when divided into Symp and NonS groups precluded reaching stronger statistical conclusions. Since the onset of symptoms in *Mecp2*-het mice is delayed and more variable than in males (24), with some females being asymptomatic even by 5 months of age (25), future studies should investigate the pubertal development in a larger cohort of female mice, following their symptoms into older adulthood.

The hypothalamic GnRH neurons are key regulators of gonadal hormones and hence of pubertal onset and fertility. Previous reports have shown hypothalamic dysfunction in *Mecp2*-mutant mice, including in the hypothalamic-hypophyseal-adrenal axis (8,44); and in leptin pathways (45,46). Indeed, a recent report studying *Mecp2*-mutant mice showed that, whereas the growth of most brain areas (such as neocortex and hippocampus) is delayed males and females, this growth is completely arrested in the hypothalamus, suggesting a more severe impairment of this important neuroendocrine structure (47). However, to our knowledge, our study is the first to report an increased density of GnRH neurons in the septo-hypothalamic region in *Mecp2*^{CD1}-null males. Excess of hypothalamic GnRH neurons due to enhanced survival and migration was demonstrated following deletion of neuropilin-1 in GnRH neurons in a mouse model of central precocious puberty (48).

The increased number of GnRH neurons in *Mecp2*^{CD1}-null males, however, did not lead to increased GnRH circulating content, but rather a slightly lower concentration of this hormone. In addition, and in agreement with a previous study (26), the circulating levels of testosterone were significantly lower in *Mecp2*^{CD1}-null males. Several mechanisms might explain this finding. As described, the low body weight of these males may have led to delayed puberty with hypogonadism. In circumstances of low nutrition and chronic

disease, GnRH pulsatility is impaired, with consequent functional hypogonadotropic hypogonadism and thus delayed pubertal onset. It is conceivable that loss of Mecp2 might result in increased hypothalamic GnRH neurons, but functional hypogonadism secondary to the whole-body effects of *Mecp2* deficiency might overcome this meaning that instead of precocious puberty, a phenotype of delayed puberty is seen in this model. In keeping with this, it is interesting that *Mecp2*^{CD1}-null males show pubertal onset at a lower body weight than healthy males.

In terms of the mechanism by which loss of *Mecp2* could affect GnRH neurons, this might occur through a dysregulation of Erα signaling, which is regulated by MeCP2 (23). The loss of *Mecp2* could also affect cells upstream of GnRH, for example, via arcuate nucleus kisspeptin modulation of GnRH release. As described, MECP2 colocalises with the histone mark H3K27me3. Enhanced H3K27me3 content at the 5′ regulatory region of the Kiss1 gene silences its expression (19), whilst reduction leads to increased Kiss1 expression, GnRH pulsatility and pubertal development. Male mice with disrupted *Kiss1* expression show a reduction in testis size as well as lower levels of testosterone (49).

Additionally, a study using a mouse model of *MECP2* duplication syndrome found that circulating levels of testosterone were increased in these mice (50). In these mice, it was shown that *Mecp2* was expressed in Leydig cells and led to an increase of androgen synthesis via an upregulation of the receptor for LH (LHCGR) and a reduction in aromatization to produce oestrogens (50). Although we did not find visible alterations in Leydig cells in our samples, future studies should address whether *Mecp2*^{CD1}-null males display lower levels of LHR in these cells.

In female mice, however, we did not find significant differences in number of GnRH cells. As with pubertal timing, the later onset of symptoms in *Mecp2*^{CD1}-het females might explain this difference. Further, since the MeCP2 protein is expressed in the nucleus of GnRH neurons, skewed X inactivation in these cells could contribute to different outcomes in terms of symptoms (51,52) and pubertal timing. Future studies assessing the GnRH system in older females might reveal relevant alterations.

The effects of pubertal dysregulation and altered hormonal signalling have an influence beyond the reproductive axis. Thus, brain circuits dependent on the levels of sex steroid hormones, such as the AVPergic system in males, display an aberrant configuration in *Mecp2*-null males, as seen previously (26) and in the present study. These circuits are involved in the control of emotional and social behaviour (53,54), highlighting the necessity of further investigating the mechanism by which *Mecp2* deficiency may impact their wiring, with the aim of finding novel therapeutic targets to potentially ameliorate emotional and social impairment in RTT and related conditions.

Limitations

With respect to human data, a limitation of our study is the exploratory nature of our survey among parents and carers, and lack of information on timing of the onset of puberty. However, our data closely matches the reported figures in a much larger study (9), giving reliability to the result. Regarding the mouse study, in spite of the high validity of the model, there are still a number of concerns when trying to translate animal data to humans. For example, in humans, boys usually die perinatally, and females develop the first symptoms during early infancy, whereas in mice, males display an overt phenotype around adolescence and females after young adulthood (24,25). Hence, the biological age of the animals and humans in terms of symptomatology is not comparable. Second, the pubertal markers used in the mouse do not completely match those of humans. In spite of these limitations, our data in the mouse model supports a disruption of the hypothalamic-hypophyseal-gonadal axis caused by *Mecp2* deficiency, whose mechanism warrants further investigation.

Conclusions

In this study, we found that a mouse model deficient for *Mecp2* display reduction in body weight during pubescence and dysregulated pubertal timing and function of the hypothalamic-gonadal axis. The effects found are strongly significant in males, hemizygous for the mutation, but less obvious in females, which could be related to heterozygosity leading to variable symptom onset. Further, we found a significant increase in GnRH neurons but a decrease in circulating GnRH and testosterone in males, suggesting a general malfunction of the hypothalamic-hypophyseal-gonadal axis. Since pubertal dysregulation has been observed in human patients with mutations in *MECP2*, our study can be used as a starting point to further investigate the biological mechanism by which *MECP2* dysfunction contributes to alterations in puberty.

List of abbreviations

ACSR	Associació Catalana de Síndrome de Rett
AESR	Asociación Española de Síndrome de Rett
AVP	Arginine-vasopressin
BPS	Balanopreputial separation
CPP	Central precocious puberty
DAPI	4’,6- diamino-2-fe-niindol
FSH	Follicle stimulant hormone
FXYD1	FXYD domain-containing transport regulator 1

GnRH	Gonadotropin Realising Hormone
LH	Luteinizing hormone
MDS	MECP2 duplication syndrome
MECP2	Methyl CpG-binding protein 2
NDS	Normal donkey serum
PBS	Phosphate saline solution
PFA	Parafolmaldehyde
RTT	Rett syndrome
TBS	TRIS buffered saline
VO	Vaginal opening

Availability of data

The datasets used and/or analysed during the current study are available from the corresponding author on reasonable request.

Funding

Funded by Ayudas FinRett 2022 and Subvenciones para grupos de investigación consolidados de la Conselleria de Educación, Cultura, Universidades y Empleo, Ref CIAICO/2023/027 to C.A.-P. SRH is funded by the Wellcome Trust (222049/Z/20/Z) and Barts Charity [MGU0552]. JER is funded by the British Society of Neuroendocrinology and the Society for Endocrinology. R.E.-P. is supported by a predoctoral fellowship from Conselleria de Educación, Cultura, Universidades y Empleo, Generalitat Valenciana, ACIF/2022/387. D.J.-D. is supported by a predoctoral fellowship from Conselleria de Educación, Cultura, Universidades y Empleo, Generalitat Valenciana, ACIF/2024/402.

Conflict of interests

The authors declare that they have no conflict of interests

Ethics approval and consent to participate

Parents and carers provided and signed an informed consent form, and the survey was approved by the Ethics Committee on Human Experimentation from the University of Valencia.

All experimental procedures were approved by the Committee of Ethics and Animal Experimentation of the Universitat de València and treated according to the European Union Council Directive of June 3rd, 2010 (6106/1/10 REV1) and under an animal-usage license issued by the Direcció General de Producció Agrària i Ramaderia de la Generalitat Valenciana (2022/VSC PEA/0288).

Permission to reproduce material from other sources

Not applicable

Authors' contributions

AMS performed experimental procedures, acquired images, analysed and interpreted data, prepared figures and wrote the manuscript; REP, DJD and AVT performed experiments and acquired images; JER contributed to data interpretation and writing; SRH obtained funding, designed the study, contributed to data interpretation and writing. CAP obtained funding, designed the study, performed and supervised experimental procedures, performed data analysis and wrote the manuscript. Final version of this manuscript was discussed and approved by all authors.

Acknowledgements

Authors are indebted to Paloma Sevilla-Ferrer, Carmen Tejada Cortés and Lidia Lloret-Martorell for technical assistance, to Dr Jose V. Torres-Pérez and Dr María Abellán-Álvaro for their help in a pilot study, to Rafael de Oza, from Associació Catalana de Síndrome de Rett, and Yolanda Corón and Laura Blázquez, from Asociación Española de Síndrome de Rett for their help in collecting patient data, and to Prof. Fernando Martínez García, Dr MªJosé Sánchez Catalán and Prof. Enrique Lanuza for discussion of results.

References

1. Nan X, Campoy FJ, Bird A. MeCP2 is a transcriptional repressor with abundant binding sites in genomic chromatin. Cell. 1997;88(4):471–81.
2. Chahrour M, Sung YJ, Shaw C, Zhou X, Wong STC, Qin J, et al. MeCP2, a key contributor to neurological disease, activates and represses transcription. Science (1979). 2008;320(5880):1224–9.
3. Shahbazian MD, Antalffy B, Armstrong DL, Zoghbi HY. Insight into Rett syndrome: MeCP2 levels display tissue- and cell-specific differences and correlate with neuronal maturation. Hum Mol Genet [Internet]. 2002 Jan 15;11(2):115–24. Available from: http://www.ncbi.nlm.nih.gov/pubmed/11809720
4. Smrt RD, Eaves-Egenes J, Barkho BZ, Santistevan NJ, Zhao C, Aimone JB, et al. Mecp2 deficiency leads to delayed maturation and altered gene expression in hippocampal neurons. Neurobiol Dis. 2007;27(1):77–89.
5. Moretti P, Zoghbi HY. MeCP2 dysfunction in Rett syndrome and related disorders. Current Opinion in Genetics and Development. 2006.
6. Amir RE, Van den Veyver IB, Wan M, Tran CQ, Francke U, Zoghbi HY. Rett syndrome is caused by mutations in X-linked MECP2, encoding methyl- CpG-binding protein 2. Nature Genet [Internet]. 1999;23(2):185–8. Available from: http://www.ncbi.nlm.nih.gov/cgi-bin/Entrez/referer?http://www.ncbi.nlm.nih.gov/htbin-post/Omim/getmim%3Ffield=medline_uid&search=10508514
7. Lombardi LM, Baker SA, Zoghbi HY. MECP2 disorders: From the clinic to mice and back. Vol. 125, Journal of Clinical Investigation. 2015. p. 2914–23.
8. Abellán-Álvaro M, Stork O, Agustín-Pavón C, Santos M. MeCP2 haplodeficiency and early-life stress interaction on anxiety-like behavior in adolescent female mice. J Neurodev Disord. 2021;13(1):59.
9. Killian JT, Lane JB, Cutter GR, Skinner SA, Kaufmann WE, Tarquinio DC, et al. Pubertal Development in Rett Syndrome Deviates From Typical Females. Pediatr Neurol. 2014 Dec;51(6):769–75.
10. Tsuji-Hosokawa A, Matsuda N, Kurosawa K, Kashimada K, Morio T. A Case of MECP2 Duplication Syndrome with Gonadotropin-Dependent Precocious Puberty. Horm Res Paediatr. 2017;87(4):271–6.
11. Holm VA. Rett syndrome: a case report from an audiovisual program. Brain Dev. 1985;7(3):297–9.

12. Baş VN, Çetinkaya S, Ağladıoğlu SY, Aksoy A, Gülpınar B, Aycan Z. Report of the first case of precocious puberty in Rett syndrome. J Pediatr Endocrinol Metab. 2013;26(9–10):937–9.
13. Canton APM, Tinano FR, Guasti L, Montenegro LR, Ryan F, Shears D, et al. Rare variants in the MECP2 gene in girls with central precocious puberty: a translational cohort study. Lancet Diabetes Endocrinol [Internet]. 2023 Aug;11(8):545–54. Available from: https://linkinghub.elsevier.com/retrieve/pii/S2213858723001316
14. Lopez-Rodriguez D, Franssen D, Heger S, Parent AS. Endocrine-disrupting chemicals and their effects on puberty. Best Pract Res Clin Endocrinol Metab. 2021 Sep;35(5):101579.
15. Avendaño MS, Vazquez MJ, Tena-Sempere M. Disentangling puberty: novel neuroendocrine pathways and mechanisms for the control of mammalian puberty. Hum Reprod Update. 2017 Nov 1;23(6):737–63.
16. Campbell RE, Coolen LM, Hoffman GE, Hrabovszky E. Highlights of neuroanatomical discoveries of the mammalian gonadotropin-releasing hormone system. J Neuroendocrinol. 2022 May 3;
17. Deng V, Matagne V, Banine F, Frerking M, Ohliger P, Budden S, et al. FXYD1 is an MeCP2 target gene overexpressed in the brains of Rett syndrome patients and Mecp2 -null mice. Hum Mol Genet [Internet]. 2007 Mar 15;16(6):640–50. Available from: https://academic.oup.com/hmg/article/16/6/640/611806
18. Garcia-Rudaz C, Deng V, Matagne V, Ronnekleiv OK, Bosch M, Han V, et al. FXYD1, a Modulator of Na + ,K + -ATPase Activity, Facilitates Female Sexual Development by Maintaining Gonadotrophin-Releasing Hormone Neuronal Excitability. J Neuroendocrinol [Internet]. 2009 Feb;21(2):108–22. Available from: https://onlinelibrary.wiley.com/doi/10.1111/j.1365-2826.2008.01812.x
19. Diotel N, Mérot Y, Coumailleau P, Gueguen M, Sérandour AA, Salbert G, et al. 5-hydroxymethylcytosine marks postmitotic neural cells in the adult and developing vertebrate central nervous system. Journal of Comparative Neurology. 2017 Feb 15;525(3):478–97.
20. Lee W, Kim J, Yun JM, Ohn T, Gong Q. MeCP2 regulates gene expression through recognition of H3K27me3. Nat Commun. 2020 Jun 19;11(1):3140.
21. Mellén M, Ayata P, Dewell S, Kriaucionis S, Heintz N. MeCP2 Binds to 5hmC Enriched within Active Genes and Accessible Chromatin in the Nervous System. Cell. 2012 Dec;151(7):1417–30.
22. Herbison AE, Pape JR. New Evidence for Estrogen Receptors in Gonadotropin-Releasing Hormone Neurons. Front Neuroendocrinol. 2001 Oct;22(4):292–308.

23. Westberry JM, Trout AL, Wilson ME. Epigenetic regulation of estrogen receptor α gene expression in the mouse cortex during early postnatal development. Endocrinology. 2010;
24. Guy J, Hendrich B, Holmes M, Martin JE, Bird a. A mouse Mecp2-null mutation causes neurological symptoms that mimic Rett syndrome. Nat Genet [Internet]. 2001;27(3):322–6. Available from: http://www.ncbi.nlm.nih.gov/pubmed/11242117
25. Cuitavi J, Martínez-Rodríguez E, Abellán-Álvaro M, García-Arencibia M, Santos M, Hipólito L, et al. Longitudinal Analysis in Mecp2-het Female Mice Reveals Atypical Nociceptive Behaviours. ResearchSquare; 2025.
26. Martínez-Rodríguez E, Martín-Sánchez A, Kul E, Bose A, Martínez-Martínez FJ, Stork O, et al. Male-specific features are reduced in Mecp2-null mice: analyses of vasopressinergic innervation, pheromone production and social behaviour. Brain Struct Funct [Internet]. 2020 Sep 4;225(7):2219–38. Available from: https://link.springer.com/10.1007/s00429-020-02122-6
27. Cobolli Gigli C, Scaramuzza L, Gandaglia A, Bellini E, Gabaglio M, Parolaro D, et al. MeCP2 Related Studies Benefit from the Use of CD1 as Genetic Background. PLoS One. 2016;11(4):e0153473.
28. Marco Hernández M, Benítez R, Medranda I, Pizarro C, Méndez MJ. Variaciones fisiológicas normales del desarrollo puberal: edad del inicio puberal, edad de la menarquia y talla. An Pediatr (Engl Ed) [Internet]. 2008 Aug;69(2):147–53. Available from: https://linkinghub.elsevier.com/retrieve/pii/S1695403308720253
29. Flores Gutiérrez J, Natali G, Giorgi J, De Leonibus E, Tongiorgi E. Mirtazapine treatment in a young female mouse model of Rett syndrome identifies time windows for the rescue of early phenotypes. Exp Neurol [Internet]. 2022 Jul;353:114056. Available from: https://linkinghub.elsevier.com/retrieve/pii/S0014488622000814
30. Arellano JI, Duque A, Rakic P. A coming-of-age story: adult neurogenesis or adolescent neurogenesis in rodents? Front Neurosci [Internet]. 2024 Mar 5;18. Available from: https://www.frontiersin.org/articles/10.3389/fnins.2024.1383728/full
31. Quignon C. Collection and Analysis of Vaginal Smears to Assess Reproductive Stage in Mice. Curr Protoc. 2023 Sep 19;3(9).
32. Ajayi AF, Akhigbe RE. Staging of the estrous cycle and induction of estrus in experimental rodents: an update. Fertil Res Pract. 2020 Dec 14;6(1):5.

33. Brust V, Schindler PM, Lewejohann L. Lifetime development of behavioural phenotype in the house mouse (Mus musculus). Front Zool. 2015 Dec 24;12(S1):S17.
34. Manfredi-Lozano M, Leysen V, Adamo M, Paiva I, Rovera R, Pignat JM, et al. GnRH replacement rescues cognition in Down syndrome. Science. 2022;377(6610):eabq4515.
35. Paxinos G, Franklin K. Academic Press. 2012. p. 360 p. Paxinos and Franklin's the Mouse Brain in Stereotaxic Coordinates. Available from: https://www.elsevier.com/books/paxinos-and-franklins-the-mouse-brain-in-stereotaxic-coordinates/paxinos/978-0-12-391057-8
36. Pepe G, Coco R, Corica D, Luppino G, Morabito LA, Lugarà C, et al. Endocrine disorders in Rett syndrome: a systematic review of the literature. Front Endocrinol (Lausanne). 2024 Oct 31;15.
37. De Felice C, Leoncini S, Signorini C, Cortelazzo A, Rovero P, Durand T, et al. Rett syndrome: An autoimmune disease? Autoimmun Rev. 2016 Apr;15(4):411–6.
38. Wong LC, Chen Y, Tsai S, Lin Y, Hsu C, Wang H, et al. Dietary intake and growth deficits in Rett syndrome—A cross-section study. Autism Research. 2021 Jul 31;14(7):1512–21.
39. Roende G, Petersen J, Ravn K, Fuglsang K, Andersen H, Nielsen JB, et al. Low bone turnover phenotype in Rett syndrome: results of biochemical bone marker analysis. Pediatr Res. 2014 Apr 27;75(4):551–8.
40. Knight O, Bebbington A, Siafarikas A, Woodhead H, Girdler S, Leonard H. Pubertal trajectory in females with Rett syndrome: A population-based study. Brain Dev. 2013 Nov;35(10):912–20.
41. Tarquinio DC, Motil KJ, Hou W, Lee HS, Glaze DG, Skinner SA, et al. Growth failure and outcome in Rett syndrome. Neurology. 2012 Oct 16;79(16):1653–61.
42. Ribeiro MC, MacDonald JL. Sex differences in Mecp2-mutant Rett syndrome model mice and the impact of cellular mosaicism in phenotype development. Brain Res. 2020 Feb;1729:146644.
43. Martínez-Rodríguez E, Martín-Sánchez A, Coviello S, Foiani C, Kul E, Stork O, et al. Lack of MeCP2 leads to region-specific increase of doublecortin in the olfactory system. Brain Struct Funct [Internet]. 2019 May 28;224(4):1647–58. Available from: http://link.springer.com/10.1007/s00429-019-01860-6
44. Braun S, Kottwitz D, Nuber UA. Pharmacological interference with the glucocorticoid system influences symptoms and lifespan in a mouse model of Rett syndrome. Hum Mol Genet. 2012;21(8):1673–80.

45. Torres-Andrade R, Moldenhauer R, Gutierrez-Bertín N, Soto-Covasich J, Mancilla-Medina C, Ehrenfeld C, et al. The increase in body weight induced by lack of methyl CpG binding protein-2 is associated with altered leptin signalling in the hypothalamus. Exp Physiol. 2014 Sep 29;99(9):1229–40.
46. Wang X, Lacza Z, Sun YE, Han W. Leptin resistance and obesity in mice with deletion of methyl-CpG-binding protein 2 (MeCP2) in hypothalamic pro-opiomelanocortin (POMC) neurons. Diabetologia. 2014 Jan 28;57(1):236–45.
47. Carli S, Chaabane L, De Rocco G, Albizzati E, Sormonta I, Calligaro S, et al. A comprehensive longitudinal study of magnetic resonance imaging identifies novel features of the Mecp2 deficient mouse brain. Neurobiol Dis [Internet]. 2023 May;180:106083. Available from: https://linkinghub.elsevier.com/retrieve/pii/S0969996123000979
48. Vanacker C, Trova S, Shruti S, Casoni F, Messina A, Croizier S, et al. Neuropilin-1 expression in GnRH neurons regulates prepubertal weight gain and sexual attraction. EMBO J. 2020 Oct 5;39(19).
49. d'Anglemont de Tassigny X, Fagg LA, Dixon JPC, Day K, Leitch HG, Hendrick AG, et al. Hypogonadotropic hypogonadism in mice lacking a functional *Kiss1* gene. Proceedings of the National Academy of Sciences. 2007 Jun 19;104(25):10714–9.
50. Wang YM, Wu Y, Zheng YF, Wang HY. MeCP2 duplication causes hyperandrogenism by upregulating LHCGR and downregulating RORα. Cell Death Dis. 2021 Oct 25;12(11):999.
51. Mykins M, Layo-Carris D, Dunn LR, Skinner DW, McBryar AH, Perez S, et al. Wild-type <scp>MECP2</scp> expression coincides with age-dependent sensory phenotypes in a female mouse model for Rett syndrome. J Neurosci Res [Internet]. 2023 Aug 7;101(8):1236–58. Available from: https://onlinelibrary.wiley.com/doi/10.1002/jnr.25190
52. Braunschweig D. X-Chromosome inactivation ratios affect wild-type MeCP2 expression within mosaic Rett syndrome and Mecp2-/+ mouse brain. Hum Mol Genet. 2004 Apr 28;13(12):1275–86.
53. Neumann I, Landgraf R. Balance of brain oxytocin and vasopressin: implications for anxiety, depression, and social behaviors. Trends Neurosci. 2012;35(11):649–59.
54. Otero-García M, Agustín-Pavón C, Lanuza E, Martínez-García F. Distribution of oxytocin and co-localization with arginine vasopressin in the brain of mice. Brain Struct Funct [Internet]. 2016 Sep 20;221(7):3445–73. Available from: http://link.springer.com/10.1007/s00429-015-1111-y

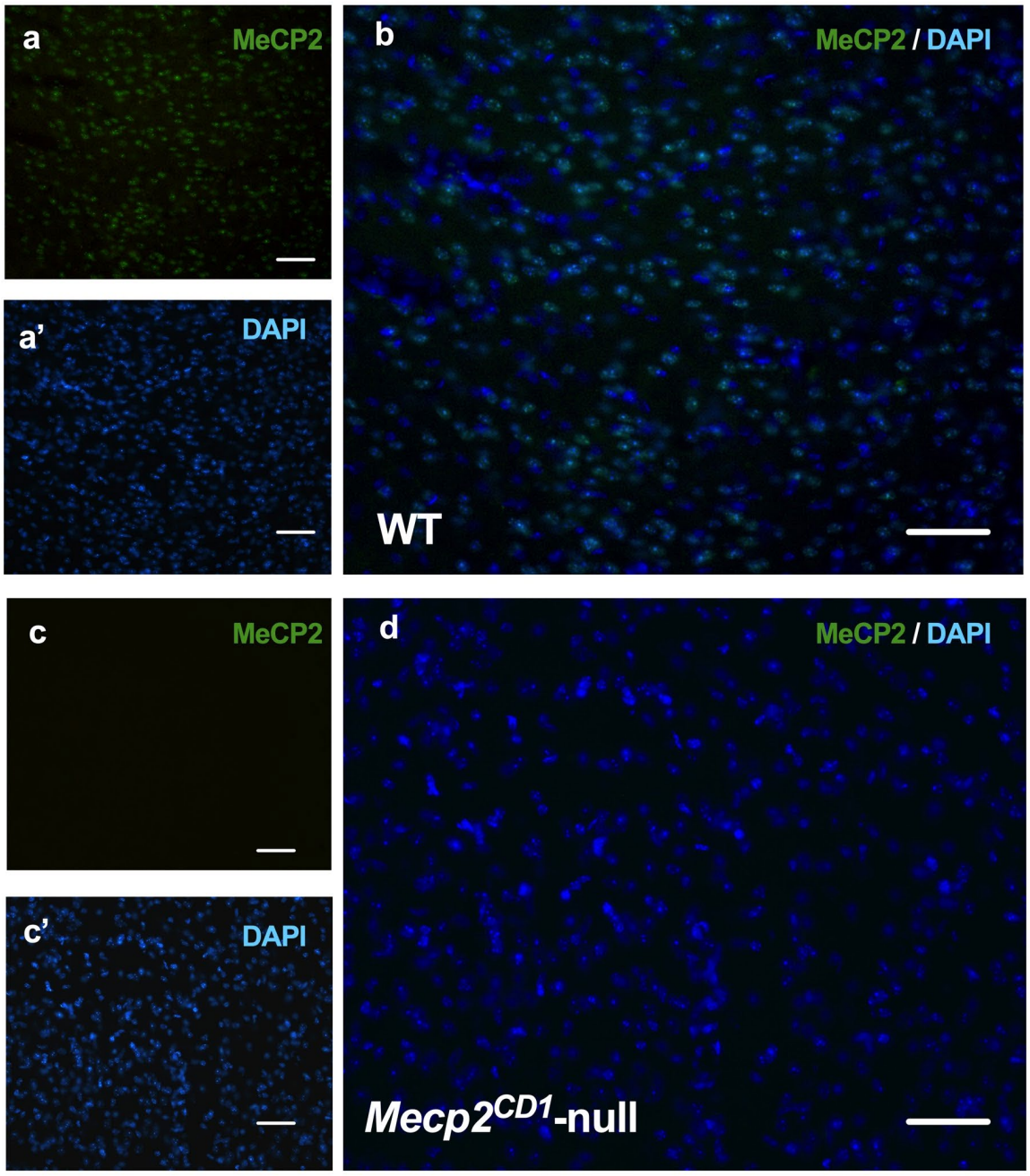

Figure S1. MeCP2 is not expressed in *Mecp2^{CD1}*-null brain tissue. Representative images of MeCP2-containing neurons (green; a and c) and DAPI (blue; a' and c') immunostained nuclei (blue) in WT and *Mecp2^{CD1}-null* mice. Noteworthy that MeCP2 expression is completely absent in *Mecp2^{CD1}-null* brain (c) tissue in comparison with WT

(a) ones, in which most of the DAPI-positive nuclei co-localize with MeCP2 signalling (b). Scale bar: 50µm.

Immunofluorescence for GnRH and MeCP2

One out of five parallel series obtained from WT (n=1) and Mecp2^{CD1}-het (n=1) females were used for simultaneous MeCP2 and GnRH immunostaining in septal-hypothalamic area sections. Free-floating sections were washed three times with 0.05 M TBS pH 7.6 (TBS). In brief, sections were (i) previously treated with citrate buffer 0.01M pH 7.6 for 30 min at 80ºC. Then, sections were (ii) pre-incubated in 3% NDS in 0.05 M TRIS buffered saline pH 7.6 (TBS) with 0.3% Triton X-100, at RT for 1 h, to block nonspecific labelling; (iii) incubated in primary antibodies, rabbit anti-GnRH primary antibody (1:5000, Invitrogen, AB1567) and mouse anti-MeCP2 (Invitrogen, MA5-33096; 1:1000) diluted in TBS with 0.3% Triton X-100 with 4% NDS at 4ºC for 48 h; (iv) incubated with fluorescent-labelled secondary antibodies (Alexa Fluor 488 donkey anti-mouse 1:400; Invitrogen A21202 and Rhodamine Red-X donkey anti-rabbit 1:400; Jackson ImmunoResearch, 711- 295-152) diluted in TBS for 2 h at RT. (v) To reveal the cytoarchitecture in brain sections, they were counterstained prior to mounting by bathing them for 1 min in DAPI (a nuclear staining) at RT. After each step, sections were washed three times for 5 min in TBS except between steps (ii) and (iii). Finally, sections were washed in TB, mounted onto gelatinised slides and cover-slipped with fluorescence mounting medium FluorSave Reagent (Sigma-Aldrich, 345789).

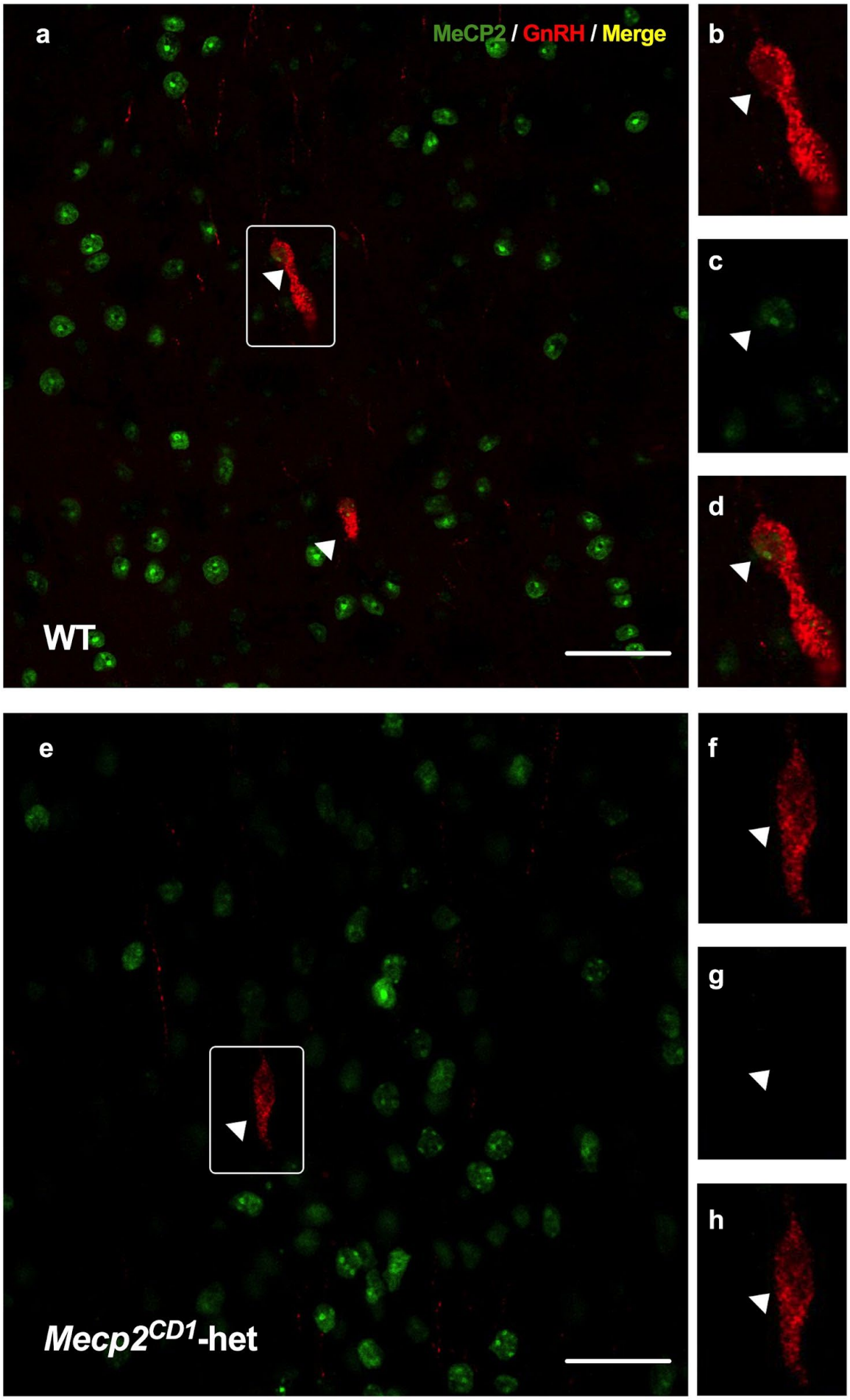
a
MeCP2 / GnRH / Merge
WT
b
c
d
e
f
g
h
Mecp2CD1-het

Figure S2. Co-localization of MeCP2 and GnRH-ir neurons in septo-hypothalamic area.

Representative single confocal plane of MeCP2-containing (green; c and g) and GnRH-containing (red; b and f) neurons. Noteworthy that MeCP2 signalling co-localizes with GnRH (a and d) in WT female septo-hypothalamic area (Bregma 0.5-0.02 mm), whereas the GnRH-ir cell did not express MeCP2 (e and h) in *Mecp2*^{CD1}-het female. Scale bar: 50µm.

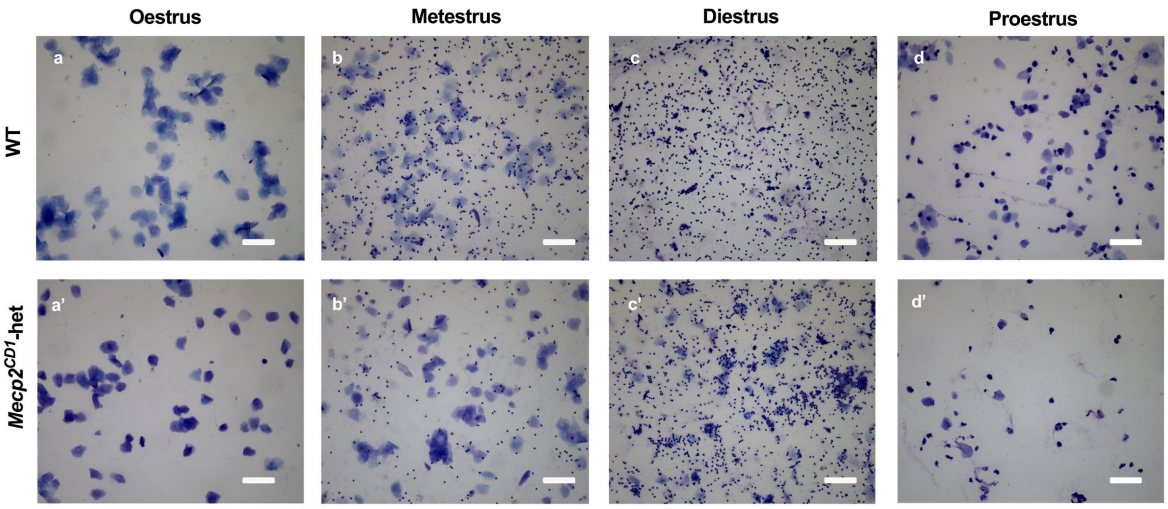

Figure S3. Photomicrographs of toluidine blue-stained vaginal smears from *Mecp2*^{CD1}-het and WT females at different phases of the oestrus cycle. a, a') Oestrus, showing almost exclusively cornified cells; (b, b') metestrus is characterised by the presence of a mix of cell types, mostly cornified cells and leukocytes, which are predominant in (c,c') diestrus phase and (d,d') proestrus, showing a high proportion of nucleated epithelial cells. Scale bar: 50µm.